

## **Supporting Information**

### **Locking of CO<sub>2</sub> in a Bio-inspired Porous-Organic-Polymeric Prison: Impact of Aliphatic Odd-Even Linker Combination**

Nitumani Das,<sup>†,§,¥</sup> Chandan Biswas,<sup>θ,§,¥</sup> Sai Vikrama Chaitanya Vummaleti,<sup>#</sup> Tahereh Azizivahed,<sup>‡</sup> Yining Huang,<sup>‡</sup> Wenjing Wang,<sup>‡,\*</sup> Xinglong Zhang,<sup>Δ,#,\*</sup> John Mondal<sup>θ,§,\*</sup>

<sup>†</sup>Department of Catalysis & Fine Chemicals, CSIR-Indian Institute of Chemical Technology, Uppal Road, Hyderabad-500 007, India.

<sup>θ</sup>Department of Organic & Medicinal Chemistry, CSIR-Indian Institute of Chemical Biology, 4 Raja S. C. Mullick Road, Jadavpur, Kolkata- 700032, India; Email:

[johnmondal@iicb.res.in](mailto:johnmondal@iicb.res.in); [johncuchem@gmail.com](mailto:johncuchem@gmail.com)

<sup>§</sup>Academy of Scientific and Innovative Research (AcSIR), Ghaziabad- 201002, India.

<sup>#</sup>Institute of High-Performance Computing (IHPC), Agency for Science, Technology and Research (A\*STAR), 1 Fusionopolis Way, #16-16 Connexis, Singapore, 138632, Singapore.

<sup>‡</sup>Department of Chemistry, University of Western Ontario, London, Ontario N6G 2V4, Canada

<sup>Δ</sup>State Key Laboratory of Structural Chemistry, Fujian Institute of Research on the Structure of Matter, Chinese Academy of Sciences, Fuzhou 350002, China; Email:

[wjwang@fjirsm.ac.cn](mailto:wjwang@fjirsm.ac.cn)

<sup>θ</sup>Department of Chemistry, The Chinese University of Hong Kong, Shatin, New Territories, Hong Kong 999077, Special Administration Region of the People's Republic of China;

Email: [xinglong.zhang@cuhk.edu.hk](mailto:xinglong.zhang@cuhk.edu.hk)

\*Corresponding Authors

<sup>¥</sup>These two authors have equally contributed in this work.

## Table of Contents

<b>Entry</b>	<b>Content</b>	<b>Page No.</b>
<b>1.</b>	Material & methods	S3
<b>2.</b>	Characterization techniques	S5
<b>3.</b>	Estimation of the isosteric heats of CO <sub>2</sub> gas adsorption ( $Q_{st}$ )	S6
<b>4.</b>	Calculation of CO <sub>2</sub> /N <sub>2</sub> selectivity based on IAST	S6
<b>5.</b>	Elemental analysis	S8
<b>6.</b>	Thermogravimetric analysis (TGA)	S9
<b>7.</b>	Stability test of <b>LPOP-n</b> using PXRD	S10
<b>8.</b>	Stability test of <b>LPOP-n</b> using FT-IR	S15
<b>9.</b>	Field emission scanning electron microscopy (FESEM) images	S20
<b>10.</b>	Transmission electron microscopy (TEM) images	S21
<b>11.</b>	Contact angle measurement of <b>LPOP-n</b> (a-e), respectively	S22
<b>12.</b>	Wide-angle powder X-ray diffraction (PXRD) pattern of <b>LPOP-2a</b>	S23
<b>13.</b>	FT-IR spectroscopy analysis of <b>LPOP-2a</b>	S24
<b>14.</b>	N <sub>2</sub> adsorption/desorption isotherm of <b>LPOP-2a</b>	S25
<b>15.</b>	Langmuir fitting of CO <sub>2</sub> adsorption isotherms	S26
<b>16.</b>	Isosteric heat of adsorption ( $Q_{st}$ )	S31
<b>17.</b>	CO <sub>2</sub> adsorption/desorption isotherms of <b>LPOP-2a</b>	S32
<b>18.</b>	Comparison study with previously reported adsorbents	S33
<b>19.</b>	Cyclic stability test of <b>LPOP-2</b>	S34
<b>20.</b>	Computational details	S35
<b>21.</b>	References	S40

## Computational Details

### Section S1: Computational methods for mechanism studies

Geometry optimizations in the gas phase were initially carried out using the global hybrid functional M06-2X<sup>5</sup> with Karlsruhe-family basis set of double- $\zeta$  valence def2-SVP<sup>6,7</sup> for all atoms as implemented in *Gaussian 16* rev. A.03.<sup>7</sup> Minima on the potential energy surface (PES) were confirmed as such by harmonic frequency analysis, showing zero imaginary frequency, at the same level of theory.

To refine the energetics, single point (SP) corrections were performed in the gas phase using M06-2X functional and def2-TZVP<sup>5,6</sup> basis set for all atoms. Gibbs energies were evaluated at the room temperature, as was used in the experiments, using a quasi-RRHO treatment of vibrational entropies. Vibrational entropies of frequencies below 100 cm<sup>-1</sup> were obtained according to a free rotor description, using a smooth damping function to interpolate between the two limiting descriptions.<sup>8</sup> M06-2X/def2-TZVP//M06-2X/def2-SVP Gibbs energies are given and quoted in kcal mol<sup>-1</sup> throughout. *Unless otherwise stated, these corrected values are used for discussion throughout the main text and in this supporting information.* All molecular structures were visualized using *PyMOL* software.

### Section S2: Conformational considerations

For the dimer model system, we initially obtained the DFT-optimized structures of **dimer-LPOP-n** ( $n = 1\text{--}5$ ) complexes at the M06-2X/def2-SVP level of theory. Subsequently, we utilized these DFT-optimized structures as input to conduct thorough conformational sampling at GFN2-xTB<sup>9–11</sup> level of theory using the CREST program version 2.12 by Grimme and co-workers.<sup>12,13</sup> From the sampling, we extracted the ten lowest-energy conformers for each **dimer-LPOP-n** system (optimized at the *xtb* level), resulting in a total of 50 conformers. These *xtb*-optimized conformers were subsequently reoptimized at the DFT (M06-2X/def2-SVP) level of theory. Next, the most stable DFT-optimized conformer of each **dimer-LPOP-n** complex was used as input for additional conformational sampling with *crest*, incorporating CO<sub>2</sub> to identify the most stable **dimer-LPOP-n\_CO<sub>2</sub>** structures. From this sampling, we extracted the five lowest-energy conformers for each **dimer-LPOP-n\_CO<sub>2</sub>** system (optimized at the *xtb* level), resulting in a total of 25 conformers. These *xtb*-optimized conformers were subsequently reoptimized at the DFT (M06-2X/def2-SVP) level of theory.

For model cage system, *crest* conformational sampling was performed to identify the most stable conformers. The lowest GFN2-xTB energy structure, *crest\_best* conformer for each

**LPOP-n\_CO<sub>2</sub>**, was used, resulting in a total of 5 conformers. These *xtb*-optimized conformers were subsequently reoptimized at the DFT (M06-2X/def2-SVP) level of theory.

### Section S3: Dimer model system of LPOP-n (n = 1–5) for CO<sub>2</sub> adsorption studies

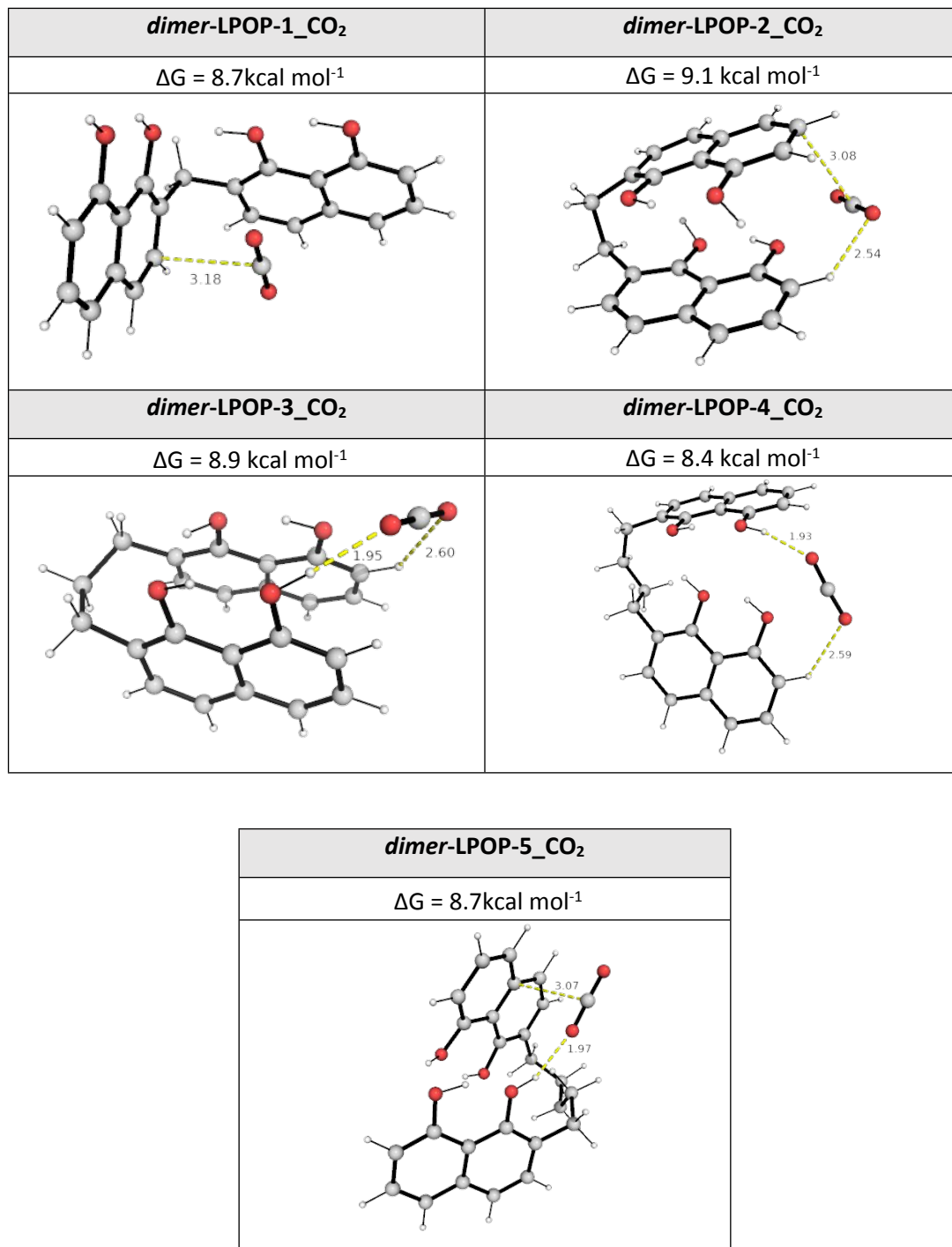


**Figure S27:** DFT optimized geometries of the studied *dimer-LPOP-n\_CO<sub>2</sub>* complexes. Key bond distances are given in Å. The CO<sub>2</sub> binding free energies ( $\Delta G_{\text{BE}}$ ) are given relative to the corresponding *dimer-LPOP-n* and CO<sub>2</sub> molecules.

## Section S4: Optimized structures and raw energies

Geometries of all optimized structures (in .xyz format with their associated energy in Hartrees) are included in a separate folder named *DFT\_optimized\_structures*. All these data have been deposited and uploaded to <https://zenodo.org/records/14870290> (DOI: 10.5281/zenodo.14870290).

Absolute values (in Hartrees) for SCF energy, zero-point vibrational energy (ZPE), enthalpy and quasi-harmonic Gibbs free energy (at 273.15K) for gas-phase M06-2X/def2-SVP optimized structures are given below. Single point corrections in gas-phase using M06-2X/def2-TZVP functional are also included.

**Table S2:** Optimized structures and raw energies.

Structure	E/au	ZPE/a u	H/au	T.S/au	qh-G/au	SP M062X/def2- TZVP
co2	-188.369743	0.010912	-188.355262	0.028007	-188.383269	-188.596318
dimer-LPOP-1_c1	-1109.555869	0.326207	-1109.212689	0.057005	-1109.266927	-1110.784672
dimer-LPOP-1_c2	-1109.548968	0.325854	-1109.205954	0.056977	-1109.260328	-1110.778951
dimer-LPOP-1_c3	-1109.548968	0.325854	-1109.205955	0.056975	-1109.260327	-1110.77895
dimer-LPOP-1_c4	-1109.548968	0.325856	-1109.205953	0.056975	-1109.260325	-1110.77895
dimer-LPOP-1_c5	-1109.547983	0.325893	-1109.204832	0.057439	-1109.259515	-1110.777585
dimer-LPOP-1_c6	-1109.546087	0.325512	-1109.203156	0.058189	-1109.258359	-1110.77648
dimer-LPOP-1_c7	-1109.545323	0.325457	-1109.202355	0.058513	-1109.257819	-1110.776013
dimer-LPOP-1_c8	-1109.545323	0.325478	-1109.202343	0.058494	-1109.257785	-1110.776017
dimer-LPOP-1_c9	-1109.545114	0.325796	-1109.201962	0.058164	-1109.257061	-1110.77477
dimer-LPOP-2_c1	-1148.820411	0.355099	-1148.447327	0.058665	-1148.503343	-1150.093132
dimer-LPOP-2_c2	-1148.817393	0.354585	-1148.444593	0.059674	-1148.501012	-1150.090706
dimer-LPOP-2_c3	-1148.819485	0.355335	-1148.446218	0.058858	-1148.502048	-1150.091105
dimer-LPOP-2_c4	-1148.819485	0.355335	-1148.446218	0.058858	-1148.502048	-1150.091105
dimer-LPOP-2_c5	-1148.819485	0.355338	-1148.446216	0.05886	-1148.502046	-1150.091106
dimer-LPOP-2_c6	-1148.821016	0.354956	-1148.448614	0.055995	-1148.502675	-1150.089995
dimer-LPOP-2_c7	-1148.813127	0.35427	-1148.440508	0.060113	-1148.497201	-1150.085626
dimer-LPOP-2_c8	-1148.813127	0.35427	-1148.440509	0.060103	-1148.497196	-1150.085624
dimer-LPOP-2_c9	-1148.813127	0.354269	-1148.440509	0.060102	-1148.497197	-1150.085623
dimer-LPOP-2_c10	-1148.813127	0.354271	-1148.440508	0.0601	-1148.497193	-1150.085623
dimer-LPOP-3_c1	-1188.094405	0.384176	-1187.691885	0.057124	-1187.747385	-1189.404365
dimer-LPOP-3_c2	-1188.094406	0.384182	-1187.691883	0.057111	-1187.747376	-1189.404362
dimer-LPOP-3_c3	-1188.090048	0.38343	-1187.687946	0.058368	-1187.744315	-1189.401987
dimer-LPOP-3_c4	-1188.090888	0.383812	-1187.688499	0.058131	-1187.744596	-1189.401455
dimer-LPOP-3_c5	-1188.086395	0.383049	-1187.684361	0.059591	-1187.741643	-1189.398468
dimer-LPOP-3_c6	-1188.086395	0.383047	-1187.684362	0.059551	-1187.741627	-1189.398462

<i>dimer-LPOP-3_c7</i>	-1188.084989	0.383369	-1187.682697	0.058961	-1187.739539	-1189.398118
<i>dimer-LPOP-3_c8</i>	-1188.084989	0.383371	-1187.682696	0.058957	-1187.739535	-1189.398118
<i>dimer-LPOP-3_c9</i>	-1188.088824	0.384143	-1187.686416	0.057348	-1187.741875	-1189.39909
<i>dimer-LPOP-3_c10</i>	-1188.088824	0.384142	-1187.686418	0.057344	-1187.741874	-1189.399087
<i>dimer-LPOP-4_c1</i>	-1227.354777	0.41247	-1226.922699	0.059656	-1226.980679	-1228.710899
<i>dimer-LPOP-4_c2</i>	-1227.352437	0.41224	-1226.920371	0.0608	-1226.978951	-1228.708758
<i>dimer-LPOP-4_c3</i>	-1227.35395	0.412718	-1226.921559	0.060197	-1226.97979	-1228.708188
<i>dimer-LPOP-4_c4</i>	-1227.350896	0.412626	-1226.918405	0.060932	-1226.977056	-1228.707804
<i>dimer-LPOP-4_c5</i>	-1227.350896	0.412632	-1226.918399	0.060933	-1226.97705	-1228.707807
<i>dimer-LPOP-4_c6</i>	-1227.353276	0.413189	-1226.920811	0.059453	-1226.978228	-1228.70753
<i>dimer-LPOP-4_c7</i>	-1227.353276	0.413189	-1226.920811	0.059453	-1226.978227	-1228.707529
<i>dimer-LPOP-4_c8</i>	-1227.353276	0.413193	-1226.920809	0.059444	-1226.97822	-1228.707528
<i>dimer-LPOP-4_c9</i>	-1227.343529	0.411874	-1226.91131	0.063431	-1226.971415	-1228.702745
<i>dimer-LPOP-4_c10</i>	-1227.345303	0.411884	-1226.913161	0.062396	-1226.972832	-1228.701697
<i>dimer-LPOP-5_c1</i>	-1266.618162	0.440932	-1266.156201	0.063655	-1266.217299	-1268.019004
<i>dimer-LPOP-5_c2</i>	-1266.617963	0.441731	-1266.155471	0.062981	-1266.215983	-1268.018031
<i>dimer-LPOP-5_c3</i>	-1266.616593	0.441137	-1266.154628	0.063102	-1266.215184	-1268.017077
<i>dimer-LPOP-5_c4</i>	-1266.615835	0.441309	-1266.153661	0.063692	-1266.214557	-1268.015701
<i>dimer-LPOP-5_c5</i>	-1266.613384	0.441043	-1266.15128	0.063895	-1266.212416	-1268.014062
<i>dimer-LPOP-5_c6</i>	-1266.612256	0.440688	-1266.150262	0.065512	-1266.212277	-1268.012854
<i>dimer-LPOP-5_c7</i>	-1266.612193	0.440665	-1266.150283	0.06505	-1266.212182	-1268.012067
<i>dimer-LPOP-5_c8</i>	-1266.611063	0.4408	-1266.149069	0.064229	-1266.210515	-1268.012391
<i>dimer-LPOP-5_c9</i>	-1266.608724	0.441026	-1266.146418	0.065495	-1266.208486	-1268.011758
<i>dimer-LPOP-5_c10</i>	-1266.603328	0.440877	-1266.141126	0.065388	-1266.203069	-1268.005178
<i>dimer-LPOP-1_CO2_c1</i>	-1297.939358	0.339339	-1297.579564	0.064751	-1297.640642	-1299.390459
<i>dimer-LPOP-1_CO2_c2</i>	-1297.941117	0.339444	-1297.58124	0.064547	-1297.642176	-1299.390324
<i>dimer-LPOP-1_CO2_c3</i>	-1297.934282	0.339328	-1297.574146	0.070352	-1297.637957	-1299.386278
<i>dimer-LPOP-1_CO2_c4</i>	-1297.934282	0.339327	-1297.574147	0.070337	-1297.637953	-1299.386279
<i>dimer-LPOP-1_CO2_c5</i>	-1297.934669	0.339002	-1297.574867	0.067435	-1297.637343	-1299.386668
<i>dimer-LPOP-2_CO2_c1</i>	-1337.208474	0.36834	-1336.819342	0.063323	-1336.88022	-1338.699712
<i>dimer-LPOP-2_CO2_c2</i>	-1337.207886	0.368182	-1336.818813	0.063641	-1336.87987	-1338.699221
<i>dimer-LPOP-2_CO2_c3</i>	-1337.206213	0.368812	-1336.816247	0.065718	-1336.878449	-1338.697531
<i>dimer-LPOP-2_CO2_c4</i>	-1337.203714	0.368665	-1336.813717	0.066575	-1336.8764	-1338.69688
<i>dimer-LPOP-2_CO2_c5</i>	-1337.205567	0.368848	-1336.815651	0.066846	-1336.878095	-1338.69666
<i>dimer-LPOP-3_CO2_c1</i>	-1376.476926	0.39737	-1376.057506	0.067371	-1376.121185	-1378.008874
<i>dimer-LPOP-3_CO2_c2</i>	-1376.473614	0.397363	-1376.05424	0.067183	-1376.11791	-1378.006765
<i>dimer-LPOP-3_CO2_c3</i>	-1376.474025	0.397281	-1376.054681	0.066719	-1376.11819	-1378.006352
<i>dimer-LPOP-3_CO2_c4</i>	-1376.472216	0.397238	-1376.052943	0.067001	-1376.116362	-1378.005763

<i>dimer-LPOP-3_CO2_c5</i>	-1376.471817	0.397383	-1376.052571	0.065344	-1376.115392	-1378.004402
<i>dimer-LPOP-4_CO2_c1</i>	-1415.738282	0.426359	-1415.288706	0.07144	-1415.355499	-1417.31609
<i>dimer-LPOP-4_CO2_c2</i>	-1415.737419	0.425617	-1415.288659	0.068309	-1415.354038	-1417.316053
<i>dimer-LPOP-4_CO2_c3</i>	-1415.738455	0.426197	-1415.289199	0.068899	-1415.35468	-1417.31461
<i>dimer-LPOP-4_CO2_c4</i>	-1415.73667	0.425912	-1415.287504	0.068994	-1415.353312	-1417.312914
<i>dimer-LPOP-4_CO2_c5</i>	-1415.736662	0.425952	-1415.287475	0.068965	-1415.353249	-1417.312882
<i>dimer-LPOP-5_CO2_c1</i>	-1455.003652	0.454713	-1454.524556	0.072656	-1454.592945	-1456.624979
<i>dimer-LPOP-5_CO2_c2</i>	-1455.001963	0.454259	-1454.523326	0.072139	-1454.591482	-1456.623664
<i>dimer-LPOP-5_CO2_c3</i>	-1454.998815	0.454329	-1454.51997	0.072726	-1454.5885	-1456.622446
<i>dimer-LPOP-5_CO2_c4</i>	-1454.998815	0.454337	-1454.51996	0.072701	-1454.58848	-1456.622447
<i>dimer-LPOP-5_CO2_c5</i>	-1454.995907	0.454349	-1454.51689	0.073291	-1454.58574	-1456.619126
<b>LPOP-1</b>	-2295.317342	0.669675	-2294.6153	0.088385	-2294.69845	-2297.840544
<b>LPOP-1_CO2</b>	-2483.704198	0.682896	-2482.98519	0.097896	-2483.07591	-2486.446909
<b>LPOP-2</b>	-2452.362495	0.785445	-2451.5403	0.097321	-2451.63112	-2455.056655
<b>LPOP-2_CO2</b>	-2640.749011	0.798605	-2639.91013	0.105076	-2640.00783	-2643.664258
<b>LPOP-3</b>	-2609.423275	0.899961	-2608.48263	0.103514	-2608.58002	-2612.287327
<b>LPOP-3_CO2</b>	-2797.808918	0.913138	-2796.85159	0.111337	-2796.95583	-2800.893938
<b>LPOP-4</b>	-2766.445437	1.013371	-2765.38522	0.120533	-2765.49626	-2769.494297
<b>LPOP-4_CO2</b>	-2954.827162	1.027195	-2953.74986	0.128962	-2953.86768	-2958.097167
<b>LPOP-5</b>	-2923.498388	1.128017	-2922.31944	0.131747	-2922.43909	-2926.720523
<b>LPOP-5_CO2</b>	-3111.887791	1.141211	-3110.69206	0.138846	-3110.81845	-3115.330806

## References

### Full reference for Gaussian software

Gaussian 16, Revision A.03, Frisch, M. J.; Trucks, G. W.; Schlegel, H. B.; Scuseria, G. E.; Robb, M. A.; Cheeseman, J. R.; Scalmani, G.; Barone, V.; Mennucci, B.; Petersson, G. A.; Nakatsuji, H.; Caricato, M.; Li, X.; Hratchian, H. P.; Izmaylov, A. F.; Bloino, J.; Zheng, G.; Sonnenberg, J. L.; Hada, M.; Ehara, M.; Toyota, K.; Fukuda, R.; Hasegawa, J.; Ishida, M.; Nakajima, T.; Honda, Y.; Kitao, O.; Nakai, H.; Vreven, T.; Montgomery Jr., J. A.; Peralta, J. E.; Ogliaro, F.; Bearpark, M.; Heyd, J. J.; Brothers, E.; Kudin, K. N.; Staroverov, V. N.; Kobayashi, R.; Normand, J.; Raghavachari, K.; Rendell, A.; Burant, J. C.; Iyengar, S. S.; Tomasi, J.; Cossi, M.; Rega, N.; Millam, J. M.; Klene, M.; Knox, J. E.; Cross, J. B.; Bakken, V.; Adamo, C.; Jaramillo, J.; Gomperts, R.; Stratmann, R. E.; Yazyev, O.; Austin, A. J.; Cammi, R.; Pomelli, C.; Ochterski, J. W.; Martin, R. L.; Morokuma, K.; Zakrzewski, V. G.; Voth, G. A.; Salvador, P.; Dannenberg, J. J.; Dapprich, S.; Daniels, A. D.; Farkas, Ö.; Foresman, J. B.; Ortiz, J. V; Cioslowski, J.; Fox, D. J. Gaussian, Inc., Wallingford CT, **2016**.

- (1) Bakhvalova, E. S.; Bykov, A. V.; Markova, M. E.; Lugovoy, Y. V.; Sidorov, A. I.; Molchanov, V. P.; Sulman, M. G.; Kiwi-Minsker, L.; Nikoshvili, L. Z. Naphthalene-Based Polymers as Catalytic Supports for Suzuki Cross-Coupling. *Molecules* **2023**, *28* (13), 4938. <https://doi.org/10.3390/molecules28134938>.
- (2) Caravatti, P.; Braunschweiler, L.; Ernst, R. R. Heteronuclear Correlation Spectroscopy in Rotating Solids. *Chem. Phys. Lett.* **1983**, *100* (4), 305–310. [https://doi.org/10.1016/0009-2614\(83\)80276-0](https://doi.org/10.1016/0009-2614(83)80276-0).
- (3) Hayashi, S.; Hayamizu, K. Chemical Shift Standards in High-Resolution Solid-State NMR (<sup>1</sup>3C, <sup>29</sup>Si, and <sup>1</sup>H Nuclei. *Bull. Chem. Soc. Jpn.* **1991**, *64*, 685–687.
- (4) Fulmer, G. R.; Miller, A. J. M.; Sherden, N. H.; Gottlieb, H. E.; Nudelman, A.; Stoltz, B. M.; Bercaw, J. E.; Goldberg, K. I. NMR Chemical Shifts of Trace Impurities: Common Laboratory Solvents, Organics, and Gases in Deuterated Solvents Relevant to the Organometallic Chemist. *Organomet.* **2010**, *29* (9), 2176–2179. <https://doi.org/10.1021/om100106e>.
- (5) Zhao, Y.; Truhlar, D. G. The M06 Suite of Density Functionals for Main Group Thermochemistry, Thermochemical Kinetics, Noncovalent Interactions, Excited States, and Transition Elements: Two New Functionals and Systematic Testing of Four M06-Class Functionals and 12 Other Function. *Theor. Chem. Acc.* **2008**, *120* (1–3), 215–241. <https://doi.org/10.1007/s00214-007-0310-x>.
- (6) Weigend, F.; Ahlrichs, R. Balanced Basis Sets of Split Valence, Triple Zeta Valence and Quadruple Zeta Valence Quality for H to Rn: Design and Assessment of Accuracy. *Phys. Chem. Chem. Phys.* **2005**, *7* (18), 3297. <https://doi.org/10.1039/b508541a>.
- (7) Weigend, F. Accurate Coulomb-Fitting Basis Sets for H to Rn. *Phys. Chem. Chem. Phys.* **2006**, *8* (9), 1057. <https://doi.org/10.1039/b515623h>.

- (8) Frisch, M. J.; Trucks, G. W.; Schlegel, H. B.; Scuseria, G. E.; Robb, M. A.; Cheeseman, J. R.; Scalmani, G.; Barone, V.; Petersson, G. A.; Nakatsuji, H.; Li, X.; Caricato, M.; Marenich, A. V.; Bloino, J.; Janesko, B. G.; Gomperts, R.; Mennucci, B.; Hratch, D. J. Gaussian 16, Revision B.01. **2016**.
- (9) Luchini, G.; Alegre-Requena, J. V.; Funes-Ardoiz, I.; Paton, R. S. GoodVibes: Automated Thermochemistry for Heterogeneous Computational Chemistry Data. *F1000Res.* **2020**, 9, 291. <https://doi.org/10.12688/f1000research.22758.1>.
- (10) Bannwarth, C.; Ehlert, S.; Grimme, S. GFN2-XTB—An Accurate and Broadly Parametrized Self-Consistent Tight-Binding Quantum Chemical Method with Multipole Electrostatics and Density-Dependent Dispersion Contributions. *J. Chem. Theory Comput.* **2019**, 15 (3), 1652–1671. <https://doi.org/10.1021/acs.jctc.8b01176>.
- (11) Grimme, S.; Bannwarth, C.; Shushkov, P. A Robust and Accurate Tight-Binding Quantum Chemical Method for Structures, Vibrational Frequencies, and Noncovalent Interactions of Large Molecular Systems Parametrized for All Spd-Block Elements (Z = 1–86). *J. Chem. Theory Comput.* **2017**, 13 (5), 1989–2009. <https://doi.org/10.1021/acs.jctc.7b00118>.
- (12) Bannwarth, C.; Caldeweyher, E.; Ehlert, S.; Hansen, A.; Pracht, P.; Seibert, J.; Spicher, S.; Grimme, S. Extended Tight-Binding Quantum Chemistry Methods. *Wiley Interdiscip. Rev., Comput. Mol. Sci.* **2021**, 11 (2), e1493. <https://doi.org/10.1002/wcms.1493>.
- (13) Grimme, S. Exploration of Chemical Compound, Conformer, and Reaction Space with Meta-Dynamics Simulations Based on Tight-Binding Quantum Chemical Calculations. *J. Chem. Theory Comput.* **2019**, 15 (5), 2847–2862. <https://doi.org/10.1021/acs.jctc.9b00143>.
- (14) Pracht, P.; Bohle, F.; Grimme, S. Automated Exploration of the Low-Energy Chemical Space with Fast Quantum Chemical Methods. *Phys. Chem. Chem. Phys.* **2020**, 22 (14), 7169–7192. <https://doi.org/10.1039/C9CP06869D>.